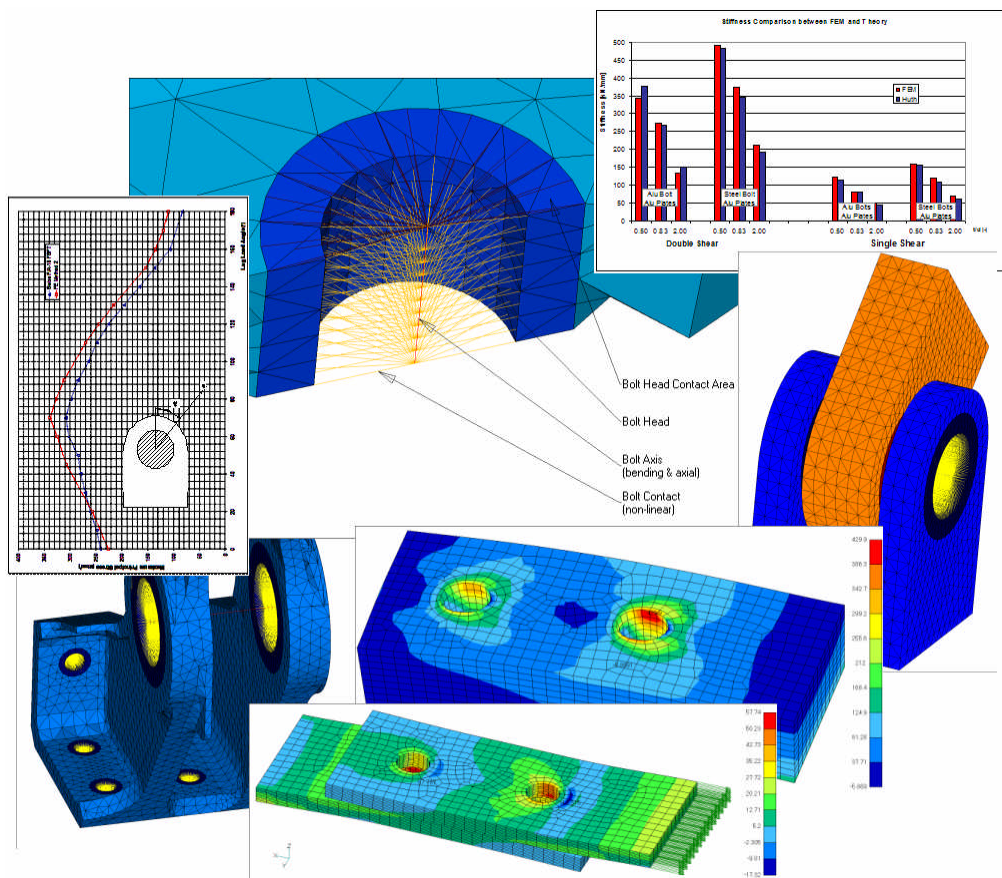


# Thierry Stehlin Dipl. Ing. ETH Structural Analysis Office

## POSTER PRESENTATION AT THE ICAF 2003

### FATIGUE ANALYSIS OF RIVETED OR BOLTED CONNECTIONS USING THE FINITE ELEMENT METHOD



**Date** : 26 April 2003

**Author** : Thierry Stehlin

**Company:** Thierry Stehlin Dipl. Ing. ETH  
Structural Analysis Office

**Address** : Obstgartenstrasse 22  
8136 Gattikon  
Switzerland

**Web Site** : [www.stehlin-engineering.ch](http://www.stehlin-engineering.ch)

## ERRATA

### Typing error in bolt flexibility equation in Chapter 4.4

Correct equation is:

$$C = \frac{b}{n} \times \left( \frac{t_1 + t_2}{2d} \right)^a \left( \frac{1}{t_1 E_1} + \frac{1}{nt_2 E_2} + \frac{1}{2t_1 E_b} + \frac{1}{2nt_2 E_b} \right)$$

C = fastener flexibility

d = fastener diameter

E = Young modulus

t = Plate thickness

single shear : n = 1

double shear : n = 2

In case of double shear  $t_1$  is the thickness of the female part and  $t_2$  is the thickness of the male part

bolted metallic joints:            a = 2/3            b = 3.0

riveted metallic joints:        a = 2/5            b = 2.2

bolted graphite/epoxy joints: a = 2/3            b = 4.2

# FATIGUE ANALYSIS OF RIVETED OR BOLTED CONNECTIONS USING THE FINITE ELEMENT METHOD

## ABSTRACT

The determination of the crack initiation life of a riveted or bolted connection requires a precise computation of the stress distribution around the critical fastener holes. For simple joint configurations, such as tension lap joints and lugs, and under certain conditions, the analysis can be performed by hand with an acceptable accuracy. For more complex joints this task can be very time consuming and the simplifications introduced in the hand calculation methods can lead to inaccurate results, or even worst, to false life predictions. Moreover, a comparison between several sources found in the literature has shown that for a same joint configuration big differences can be obtained in the maximum stress prediction (up to a factor of 2). The consequence is that, depending on the source used, extremely different results in the fatigue strength assessment of a connection are obtained. This unsatisfactory situation as well as the need for a more universal analysis technique, which can be used on a wide range of joints geometry, motivated the development of an analysis method based on the Finite Element Method.

## NOTATION

a	fastener edge distance
d	fastener diameter
e	fastener-to-hole clearance as a percentage of d
t	plate thickness
$A_{\text{bar}}$	bar element area
$A_{\text{rod}}$	rod element area
C	fastener flexibility
E	Youngs modulus
$I_{\text{bar}}$	bar element moment of inertia
$K_t$	lug net stress concentration factor
$K_{\text{tp}}$	pin bending factor
$N_{\text{rod}}$	number of rod elements per fastener
W	lug width
$\lambda_{\text{assy}}$	assembly compliance
$\theta$	load angle
SN	Stress-life
$\epsilon N$	Strain-life

## 1 INTRODUCTION

The fatigue strength assessment of joints is a complex process, which includes various engineering fields, such as load time history assessment, material data knowledge, tests definition and interpretation, load path assessment within the structure and detailed stress distribution computation. The stress distribution assessment within the connected parts and the maximum stress computation around the fastener holes are the subject of this paper.

Over the past decades, conventional hand calculation methods have been developed to compute the maximum stress around holes loaded by fasteners and bypassing loads. These methods are based on curves presenting the stress concentration factors, which are to be applied to the bearing stress or the net stress in function of the joint/plate geometry for standard loading cases. In real joints the load transferred by each fastener is reacted

partly by shear and partly by tension within the connected parts. The task of the stress engineer is to assess how much of the bearing load is reacted by tension and by shear respectively, and to determine the gross thru stress and shear stress within the connected parts (also called bypassing stresses). In other words, the goal is to breakdown the complex stress field into several standard loading cases, for which it is possible to compute the stress distribution around the hole using the curves mentioned above and then combine the results to compute the maximum principal stress at the critical location. A typical example showing the procedure described above is presented in Figure 1. All cases mentioned above, if looked at separately, lead to a maximum stress concentration at different positions around the hole. This makes the analysis more complex. Therefore, this procedure is difficult and time consuming. In addition, secondary effects, such as local out-of-plane bending and tension of the fastener can occur. In these instances, it is very difficult to compute the stress around the hole using conventional hand calculation techniques and these effects are usually neglected. Unfortunately, this can lead to inaccurate results.

The stress distribution and the maximum principal stress around a fastened hole can be computed by hand with an acceptable accuracy for “simple” connections, such as tension lap joints or lugs, when the ratio plate thickness over bolt/rivet diameter ( $t/d$ ) is below 0.5. For higher  $t/d$ , stress peaking due to pin bending will occur at the faying surface (see Figure 2). The peaking factor ( $K_{tp}$ ) depends on many factors such as the lug geometry, pin and lug modulus of elasticity and the out-of-plane restraint of the connected parts. The curves for the assessment of  $K_{tp}$  found in literature show a large scatter between the different sources. This, in turn, leads to very different results in the fatigue strength assessment.

The method presented in this paper permits to assess firstly the load distribution within the fasteners in multiple fastener joints and secondly the stress distribution around each fastener hole in one analysis loop. Note that the fasteners do not necessarily need to lie within one plane and that any 3D bolting configurations can be modelled. The goal is to keep the model complexity to a minimum and to avoid the use of contact or gap elements. These elements can lead to severe convergence problems and high computational time.

The FE method presented uses the following elements with properties adapted to the fastener type and material:

- a) solid elements for the connected parts
- b) bar elements for the fasteners
- c) rod elements for the interaction between the fasteners and the connected parts
- d) rigid elements for the fasteners head

In order to simulate the contact between the fastener and the connected parts, non-linear material properties are used for some elements, i.e. zero stiffness in tension and fastener material modulus in compression. This modelling method is easy to implement in FEM with today’s pre-processors and it shows a rapid convergence of the solution.

## 2 CONVENTIONAL CALCULATIONS

In conventional calculations of bolted/riveted joints, the first step is to define the critical location by computing the load distribution within the fasteners. This can be performed by hand, by using dedicated computer programs or by the finite element method using, for example, plate elements for the connected parts and spring elements for the fasteners. The second step is to define the global stress field in the vicinity of the hole and to assess how much of the load transferred by the fastener is reacted by shear and how much is reacted by tension within the connected parts (see Figure 1). The third step is to compute the maximum stress around the hole accounting for the effects mentioned above. This step can be performed “manually” or can be automated in computer programs. Whichever of the methods is used, the maximum stress computation is usually based on curves, which can partly be found in literature. A comparison between several different sources is presented in the following.

Figure 3 shows the stress concentration factor in square-ended lugs ( $K_t$ ) in function of the lug geometry as a comparison between references [1], [2] and [3]. The curves are based on an edge distance over lug width ratio ( $a/W$ ) of 0.5 and present  $K_t$  in function of the fastener diameter over lug width ratio ( $d/W$ ). The curves show a very good agreement between the different sources with differences remaining below 10%.

Figure 4 shows the pin bending factor ( $K_{tp}$ ) in function of the plate thickness over fastener diameter ratio ( $t/d$ ) as a comparison between references [1], [2] and [3]. It is interesting to pick out that references [1] and [3] account for the plate and fastener modulus, but do not differentiate between single shear and double shear lap joints, while [2] accounts for the joint configuration, i.e. single shear or double shear, but does not account for the plate

and fastener modulus. Also note that in references [1] and [2] the given curves are valid only for certain conditions and are presented as a guide for preliminary design. Moreover, [2] strongly recommends the use of a computer to assess the stress distribution around the fastener hole.

The curves presented in Figure 4 show very large discrepancies (up to 200%) in the  $K_{ip}$ . This is definitely not acceptable on a fatigue analysis point of view, where small stress differences can lead to huge scatter in life calculation.

## 3 FEM DESCRIPTION

### 3.1 Detailed Model of the Connection (“FE Method 1”)

A very detailed way to model a bolted/riveted connection is to use solid elements to idealize the plates and fasteners, and to use gap/contact elements to account for the interaction between the fasteners and the connected plates (see Figure 5).

In practice, when connections including several bolts/rivets have to be analysed, this way of modelling can lead to severe convergence problems (MSC/NASTRAN solver). Moreover, high computational time is necessary to find a solution because the use of gap element requires many small load steps during the iteration process. Therefore, this way of modelling is definitely not adapted to development projects, which require short design loops and quick responses to the problems.

However, the author believes that this is one of the most exact methods available today to model these types of joints. Therefore, this modelling method, called herein FE Method 1, will be used as reference for the validation of the simplified FE method (herein FE Method 2) described below.

### 3.2 Simplified Model of the Connection (“FE Method 2”)

As for FE Method 1, the plates are idealized using solid elements. The bolts/rivets are idealized by bar elements to simulate the fastener axial and bending behavior and by rod elements to simulate the load transfer between the bolts and the connected plates. The bar elements are positioned along the fastener axis and have the E-modulus of the fastener material and the axial and bending properties of the fastener ( $A_{bar}=\pi d^2/4$  respectively  $I_{bar}=\pi d^4/64$ ). When a preload is applied to the assembly, the bar axial properties are modified to account for the assembly compliance  $\lambda_{assy}$  ( $A_{bar}=1/\lambda_{assy} \cdot \pi d^2/4$ , with  $\lambda_{assy} \leq 1.0$ ). The fastener axis is connected to the plate by means of radial rod elements, which lie in equidistant planes perpendicular to the plate bolt axis. The area of the rod elements ( $A_{rod}$ ) is defined in such a way so that the sum of the area of the rods used to model one bolt represents the area of the hole surface or, in other words,  $A_{rod}=\pi dt/N_{rod}$  with  $N_{rod}$  being the number of rod elements used. The rod elements have non-linear properties to account for the contact between the fastener and the plate, i.e. zero stiffness in tension and the E-modulus of the fastener material in compression.

A rigid element (RBE2 in MSC/NASTRAN) on the bolt head side is used to simulate the bolt head, i.e. to ensure the axial load and the local bending moment transfer between the fastener and the plate. The plate surface area used to react these axial and bending loads is equal to the fastener head contact area.

Another rigid element (RBE2) is used on the contact surface of each connected plates. These elements connect the out-of-plane degree of freedom of the nodes at the plates contact surfaces in order to avoid excessive local deformation around the holes and to account for the restraint provided by the contact between the plates. These elements are only used when the connected parts are forced to stay in contact, for example when a pretension is applied to the fastener. In the case of lugs with a gap between the male and female parts, these elements are not used.

Note that the use of non-linear rod elements instead of gap elements to idealize the interaction between the fasteners and the plates minimizes the convergence problems and reduces the computational time by a factor 2 to 10, because much less load increment steps are required to find the solution.

An example of FE Method 2 mesh is presented in the Figure 6.

### 3.3 Single Lap Joint Mesh for analysis study

A typical single lap joint FE model is shown in Figure 7. Because no out-of-plane restraint is provided, two bolts are needed to react the local bending coming from the offset between the plates. The bolts are constrained in rotation about their axis to avoid excessive rotation of the bar elements, which could lead to numerical problems. One plate is clamped at its end (no translation and no rotation), while the other plate end, where the tension loading is applied, is restrained in rotation (see Figure 8). This kind of model has been used for the computation of the pin bending effect ( $K_{tp}$ ) and of the joint stiffness for single lap joints configuration. The single lap joint model should provide a higher bound for  $K_{tp}$  since no out-of-plane restraint is applied to the connection.

### 3.4 Double Lap Joint Mesh for analysis study

A typical double lap joint FE model is shown in the Figure 9. The male plate is clamped at its end (no translation and no rotation), while the female plate end, where the tension loading is applied, is restrained in rotation (see Figure 10). Symmetry boundary conditions are applied at the symmetry plane (male plate mid-plane). Out-of-plane restraint is applied at the female plate outer surface to avoid bending of the plate. The bolt is constrained in rotation about its axis to avoid excessive rotation of the bar elements, which could lead to numerical problems. This kind of model has been used for the computation of the pin bending effect ( $K_{tp}$ ) and of the joint stiffness for double lap joints configuration. The double lap joint model should provide a lower bound for  $K_{tp}$  since the connection is hold flat (no out-of-plane deformation is possible).

## 4 RESULTS

### 4.1 Lug Net Stress Concentration $K_t$

The lug net stress concentration factors for square-ended lugs have been computed using FE models similar to the model shown in Figures 11 and 12. The  $a/W$  ratio (edge distance to lug width) has been kept constant at 0.5, while the  $d/W$  ratio (pin diameter to lug width) has been varied from 0.2 to 0.7.

Figure 13 shows the comparison of the computed net stress concentration between the FE Method 1 and FE Method 2. A very good agreement is demonstrated with differences lower than 3%.

Figure 14 shows a comparison between the curves presented in references [1], [2] & [3] and the FE Method 2. They correspond well. The differences lie between 0% and 20%, depending on which reference is taken as the basis for the comparison. Note that the FE Method leads to lower  $K_t$  than the ESDU [1] method throughout the entire  $d/W$  range (-6% to -12% difference for  $0.2 < d/W < 0.6$ ). One possible reason is explained in detail in Section 5.1.

### 4.2 Pin Bending Factor $K_{tp}$

The pin bending factor has been computed using the single lap (Figure 7), double lap (Figure 9) and male lug (Figure 12) models for different geometries. The pin bending factor is defined as the maximum stress computed around the lug hole near the faying surface in single or double lap joints divided by the maximum stress computed around the lug hole in a male lug (no load eccentricity) having the same geometry (pin diameter, edge distance, thickness and width).

Figure 15 shows a comparison of the pin bending factor between the FE Method 1 and FE Method 2. Again the two modelling methods correspond fairly well with each other.

The study has shown that the pin bending factor depends on different factors such as the  $t/d$  ratio, the out-of-plane restraint of the connection and, to a smaller extend, the  $E_p/E_1$  ratio (pin E-modulus over plate E-Modulus). The curves presented in references [1] to [3] neglect either the  $E_p/E_1$  effect or the out-of-plane restraint factor and are generally optimistic regarding to the FE results with the exception of the curve for single lap joints presented in reference [2].

The Figure 16 shows a comparison between the curves presented in [2] and the FE Method 2 curves for single lap joints and double lap joints. Both methods show the same trend in the  $K_{ip}$ , but substantial differences are observed. As previously stated, reference [2] mentions that the given curves are presented as a guide for preliminary design.

FEM studies on several other joint configurations revealed that the stiffness of the connected parts as well as the stiffness of the surrounding structure or the boundary conditions play a major role in the  $K_{ip}$  value for  $t/d > 0.5$ . This could explain the big scatter in the  $K_{ip}$  curves found in literature, which are probably not based on the same test or boundary conditions. This is a strong argument for the use of detailed FEM analysis, which is able to account for the specificity of the joint analysed.

### 4.3 Load Angle Effect

The maximum principal stress around a fastener hole is dependent on the loading direction. In other words, the maximum stress depends on the way the fastener load is reacted in the plate: tension, compression or shear.

A study have been performed on a round-ended lug with the loading angle varying from  $0^\circ$  to  $180^\circ$ . The FE model used for this study is shown in Figure 17 and the principal stress distribution for a loading angle of  $45^\circ$  is shown in Figure 18. The lug geometry was defined as the following:  $a = 55\text{mm}$ ,  $d = 54\text{mm}$ ,  $W = 110\text{mm}$  and  $t = 22.5\text{mm}$ . The lug and the pin are made of aluminium.

Figure 19 shows the computed maximum principal stress for the lug geometry described above in function of the load angle  $\theta$  using reference [3] curves and the FE Method 2. Figure 20 presents the difference in [%] between the two methods. A very good agreement has been found with a difference remaining below 10% for loading angles up to  $150^\circ$ . For loading angles between  $150^\circ$  and  $180^\circ$  the agreement is less good and the difference can reach 25%. However, at these high loading angles the maximum stress is lower by a factor 2 to 3 than at smaller loading angles. Therefore, the relative difference is higher, although the absolute difference is not bigger than for other loading angles (see Figure 21).

Note that the stress distribution and the maximum stress depend on the position of the clamping or, in case of a continuous structure, on the stiffness of the backup structure. In this study, the clamping was positioned 110 mm away from the pin axis.

### 4.4 Stiffness

In multiple fasteners joints an accurate assessment of the fastener flexibility is paramount for the determination of the joint load distribution. Several semi-empirical formulas for the calculation of fastener flexibility exist in literature. According to [4], these formulas turned out to be inaccurate or at least not applicable for a wide range of joint geometries. An extensive experimental investigation has been performed [4] during which fastener flexibilities for a wide range of joints of practical interest were determined. A formula for fastener flexibility has been derived [4] from the tests results and proved to be significantly superior to those found in literature:

$$C = \left( \frac{t_1 + t_2}{2d} \right)^a \frac{b}{n} \left( \frac{1}{t_1 E_1} + \frac{1}{n t_2 E_2} + \frac{1}{n t_1 E_3} + \frac{1}{2n t_2 E_3} \right) \quad (1)$$

with: C = fastener flexibility  
d = fastener diameter  
E = Young modulus  
t = Plate thickness

n = 1 for single shear joints  
n = 2 for double shear joints

a = 2/3; b = 3.0 for bolted metallic joints

Indices: 1 for top plate or male lug, 2 for bottom plate or female lug and 3 for fastener

Because the formula (1) corresponds very well with test results for a wide range of joints configurations, it is taken as a basis to validate the FE Method 2.

Reference [4] presents a procedure to experimentally determine the deformation of the joint. The joint was equipped with a strain gage extensometer and the elastic deformations of the specimen segments within the gage length were eliminated by electric compensation. This procedure permits to directly record the load-deformation curve.

An equivalent procedure has been used to determine the deformation of the joint in the FE model. The displacements at each end of the plates are computed; this permits to compute the total deformation of the assembly, including bolt bending, bearing deformation and plates elongation. Then the elastic deformation of the plates is subtracted to derive the deformation of the joint.

Figure 22 presents the comparison of the joint stiffness computed with Equation (1) and with the FE Method 2 for different bolted joint configurations. The agreement is very good with differences staying below 10%, thus showing that this modelling method can accurately predict the joint stiffness.

## 5 LIMITATIONS

### 5.1 Interference Fit / Clearance Fit Fasteners

The use of rod elements with non-linear properties to idealise the contact between the fasteners and the connected parts means that the gap between the fasteners and the plates is equal to zero, i.e. that a very light interference fit fastener is simulated. Thus, the FE method 2 implies that the stress relief around the hole due to the fastener stiffness is taken into account in the analysis.

The fastener-to-hole clearance significantly affects the stress concentration. Reference [1] presents a method to assess the impact of the clearance on the maximum stress. Figure 23 shows the stress concentration curves computed from Ref [1] for square-ended lugs with  $a/W = 0.5$  in function of  $d/W$  for  $e = 0.0\%$ ,  $e = 0.1\%$  and  $e = 0.2\%$ , with  $e$  being the fastener-to-hole clearance as a percentage of  $d$ . Note that the curve for  $e = 0.0\%$  is a kind of extrapolation and thus, considered as an attempt.

It is worth mentioning that a very small clearance ( $e < 0.1\%$ ) is usually only obtained in laboratory specimens, where a careful manufacturing is expected and an individual pairing of hole and fastener is performed. For this reason it is recommended to use curves with  $e = 0.2$  in the daily practice [1] when clearance fit fasteners are used.

The FE Method 1, which uses gap elements, is able to simulate fastener-to-hole clearance. Therefore, this method has been used to study the impact of the fastener-to-hole clearance on the computed stress concentration. Figure 24 shows the stress concentration curves computed by FE for square-ended lugs with  $a/W = 0.5$  in function of  $d/W$  for  $e = 0.0\%$ ,  $e = 0.1\%$  and  $e = 0.2\%$ .

A comparison between Figures 23 and 24 shows that the predicted impact of the clearance on the stress concentration is of the same order for both methods (Figure 25), i.e. the steps between the curves for  $e = 0.0\%$ ,  $e = 0.1\%$  and  $e = 0.2\%$  are similar for both methods. As a first approximation, a stress increase of 10% to 20% is expected for the  $d/W$  range of 0.2 to 0.7 when the clearance is increased from 0.0% (light interference fit) to 0.2% (clearance fit).

In order to derive a safety margin for fatigue, material data have to be used to compute the allowable fatigue stress or to predict the fatigue life of the assembly. These data are based on fatigue tests with configurations depending on the analysis approach used, global or local, i.e. stress-life (SN) or strain-life ( $\epsilon N$ ). The derivation of SN curves can be based on different test configurations such as coupons with known stress concentration factors, bolted joints with clearance fit fasteners or interference fit fasteners, riveted joints, lugs with or without bushes, etc. In the case of  $\epsilon N$  curves standardised coupons are used.

Depending on the fatigue analysis approach used and on the material data available to the engineer, the results obtained by the FE Method 2 have to be slightly adapted. In the following list, analysis procedures are proposed for different configurations, which can be encountered in practice.

1. Clearance fit fasteners and SN curves for plain material or  $\epsilon$ N curves: correct the FE results using the method presented in ESDU [1] for  $e = 0.2\%$ .
2. Interference fit fasteners or lugs with interference fit bushes or press-fit bushes and SN curves for plain material: correct the FE results using the method presented in ESDU [1] for  $e = 0.2\%$  and apply the adapted correction factor on stress or life to account for the interference fit effect. The use of the FE results and SN curves without any correction should lead to conservative results.
3. Interference fit fasteners or lugs with interference fit bushes or press-fit bushes and corresponding SN curves: use FE Method 2 results without corrections.
4. Interference fit fasteners or lugs with interference fit bushes or press-fit bushes and  $\epsilon$ N curves: correct the FE results using the method presented in ESDU [1] for  $e = 0.2\%$  and apply the adapted correction factor on stress or life to account for the interference fit effect. The use of the FE results and  $\epsilon$ N curves without any correction should lead to conservative results.
5. Riveted connection and corresponding SN curves: use FE Method 2 without corrections.
6. Lugs with clearance fit pins and corresponding SN curves: use FE Method 2 without corrections.

The list presented above is intended as guidance and does not cover all possibilities, which could arise in practice. Therefore, it is the engineer's choice to adapt his analytical approach from case to case. Note that the correction method presented in [1] is considered as an approximation and that the use of curves based on detailed FEM or tests is recommended.

## 5.2 Friction between the connected parts

According to [4], frictional forces, depending on clamping forces and changing as a results of fatigue loading, influence the maximum stress around the hole. With increasing friction, the contribution from the bearing load to the local stress decreases. Redistribution of loads or changes in the load transfer mechanisms results in a relief of the critical volume of material at the edge of the fastener hole.

The method presented in this paper as well as the conventional hand calculation methods do not account for the load transfer due to friction. Therefore, the fatigue life of connections with fasteners having a pretension cannot be accurately predicted and the results should be used with caution, except if the material data already include such a parameters (for example SN curves for lap joints with a given type of fastener with a defined pretension) or except if correction factors based on test results are applied.

# 6 PRACTICAL CONSIDERATIONS

## 6.1 TET Mesh transition

Traditionally the eight-node hexahedron element (brick element) is the preferred solid element type for performing detailed stress analysis. It is capable of representing linearly-varying displacement and stress fields within the element. Due to their brick shape, hex elements can only be generated by meshing 5 or 6-sided solids (simple solids) or by sweeping quadrilateral plate elements. A typical solid imported from a CAD package has a complex geometry (with changes of thickness, fillets, notches, etc...) and cannot be directly hex-meshed. It must first be partitioned into simple solids before it can be hex meshed. This requires planning, patience, and time. It may take a skilled structural analyst several days to manually hex-mesh a complex part. This is often not acceptable in development projects, where several design loops have to be performed in a short time. Therefore, the automatic tet mesher is preferred. Nowadays pre-processor softwares such as *Femap* or *Patran* are capable of meshing a complex solid directly to generate tetrahedron elements. It is called an "automatic" mesher because complex solid geometries can be directly tet-meshed without any prior geometry manipulation and different mesh sizes within the part can easily be defined. The elements generated by these programs are either 4-node or 10-node tetrahedron elements (TET4 or TET10 elements). The TET4 element is a constant-strain element and is not suitable for capturing the high stress gradients typically found in bolted/riveted connections. The TET10 element is a linear-strain element, which is capable of representing a linearly-varying stress field within the element. It has four corner nodes and 6 mid-side nodes. The mid-side nodes allow the TET10 element to have curved edges and faces, which enable it to capture the curved part geometry with a quadratic fit.

The modelling method presented in this paper requires a mapped mesh on the fastener hole surface in order to have equally spaced spiders of radial rod elements. The mesh transition between the mapped mesh and the tet mesh of the solid parts is automatically made by *Femap* or *Patran*, if the hole surface is mapped meshed prior to the free tetrahedron meshing.

## 6.2 Minimum node numbers around a hole

A minimum of 10 nodes over the plate thickness is required to accurately assess the pin bending effect ( $K_{tp}$ ). For standards bolted/riveted connection with  $t/d$  between 0.5 and 2.0 a minimum of 20 nodes along the hole perimeter are required to ensure an accurate maximum stress computation. For lugs, where the  $t/d$  ratio can be much lower than 0.5, the number of nodes required is higher. Attention should be paid to the mesh size definition in the circumferential and transversal directions before the mapped meshing of the hole surface. The mesh size should be similar in both directions in order to minimize the element distortion. Some typical mesh used for bolted connection and lug analyses are shown in Figures 26 and 27.

The minimum nodes number mentioned above is given as a general guide and it is the stress engineer's decision if the mesh size used is fine enough to reach the desired accuracy in the analysis. A finer mesh can lead to more accurate results, but at the cost of computational time. For example the typical number of nodes along the hole perimeter in the studies presented in this paper was 20. Several runs have been performed using 40 nodes along the hole perimeter in order to evaluate the impact of the mesh size on the analysis accuracy as well as on the computational time. The difference in the maximum stress computation was below 10%, while the analysis time almost doubled.

## 6.3 Model Size

When the connected parts are meshed with solid elements, the model size can easily become very large. This means time intensive meshing and analysis. In several cases, it is possible to minimise the model size by modelling the critical part with solid elements and the other part with shell elements. Thus, the stiffness of the backup structure is accounted for in the analysis with a minimum impact on the model size.

# 7 CONCLUSIONS

The computation of the maximum stress in bolted/riveted joints can be preformed either by using hand calculation methods or by developing a detailed FEM of the assembly using gap elements (FE Method 1) to account for the fastener to connected parts interaction. Both methods have their advantages and disadvantages.

The hand calculation methods are quick and easy to use, but they are limited to simple load cases, such as tension in lugs or lap joints. Further they are limited to certain geometrical configurations. They can be extrapolated to more complex joints, but in this case the analysis can be time consuming and the simplifications introduced can lead to rough results. Moreover, a comparison between sources [1], [2] and [3] has shown big discrepancies (up to a factor of 2) in the assessment of the pin bending effect, which becomes very important when  $t/d > 0.5$  (plate thickness over fastener diameter ratio).

The FE Method 1 is very accurate and can account for effects such as gap or interference between the fastener and the plates, local bending, fasteners stiffness, etc. However, this method can be highly time consuming because convergence problems occur when joints with several fasteners are idealized (MSC/NASTRAN solver).

A Finite Element Method based on rod elements with non-linear properties to idealize the fastener to plate interaction has been presented in this paper (FE Method 2). This method shows very similar results when compared to the Finite Element Method based on gap elements (FE Method 1). The advantage of the FE Method 2 is that the risk of convergence problems is virtually eliminated. Moreover, the computational time is considerably reduced (by a factor 2 to 10) regarding the FE Method 1, because less load increment steps are required for the solution to converge. Studies have shown that the computed maximum principal stress using the FE Method 2 is close to the maximum stress predicted using conventional hand calculation methods for several

joint configurations and geometries. In addition, the fastener flexibility is accurately predicted, thus giving a very good confidence in the load distribution assessment within multiple fasteners joints.

The FE Method 2 is very flexible and can be adapted to a lot of practical situations. It can backup the hand calculation in the case of doubts (anticipated local effects, high t/d ratio, etc.) or it obtains a solution for geometries outside the validity range of the hand calculation methods.

This method can also be applied to derive more accurate curves for the pin bending factor accounting for different configurations (end fastener in splices or stiffeners, structure hold flat, structure free to move in the out-of-plane direction, etc...). The computed curves could be adapted to the specific needs of the company or project and would drastically improve the analysis accuracy of lugs or tension splices calculated by hand for  $t/d > 0.5$ .

## **8 REFERENCES**

- [1] ESDU, Data Item 81006: Stress concentration factors of axially loaded lugs with clearance-fit pins.
- [2] Airframe Structural Design, Michael C. Y. Niu
- [3] Swiss F/A-18 FSFT
- [4] Fatigue in Mechanically Fastened Composite and Metallic Joints, ASTM STP 927  
Influence of Fastener Flexibility on the Prediction of Load Transfer and Fatigue Life for Multiple-Row Joints, Huth

## **ACKNOWLEDGEMENTS**

The author would like to thank Mr. Dr. Michel Guillaume, Dr. Arnold Schmid and Michel Godinat from RUAG Aerospace (Emmen, Switzerland) for many stimulating discussions. Thanks are also due to Dr. Peter Kupferschmied and Amélie Gottier for their review of this document and their constructive suggestions.

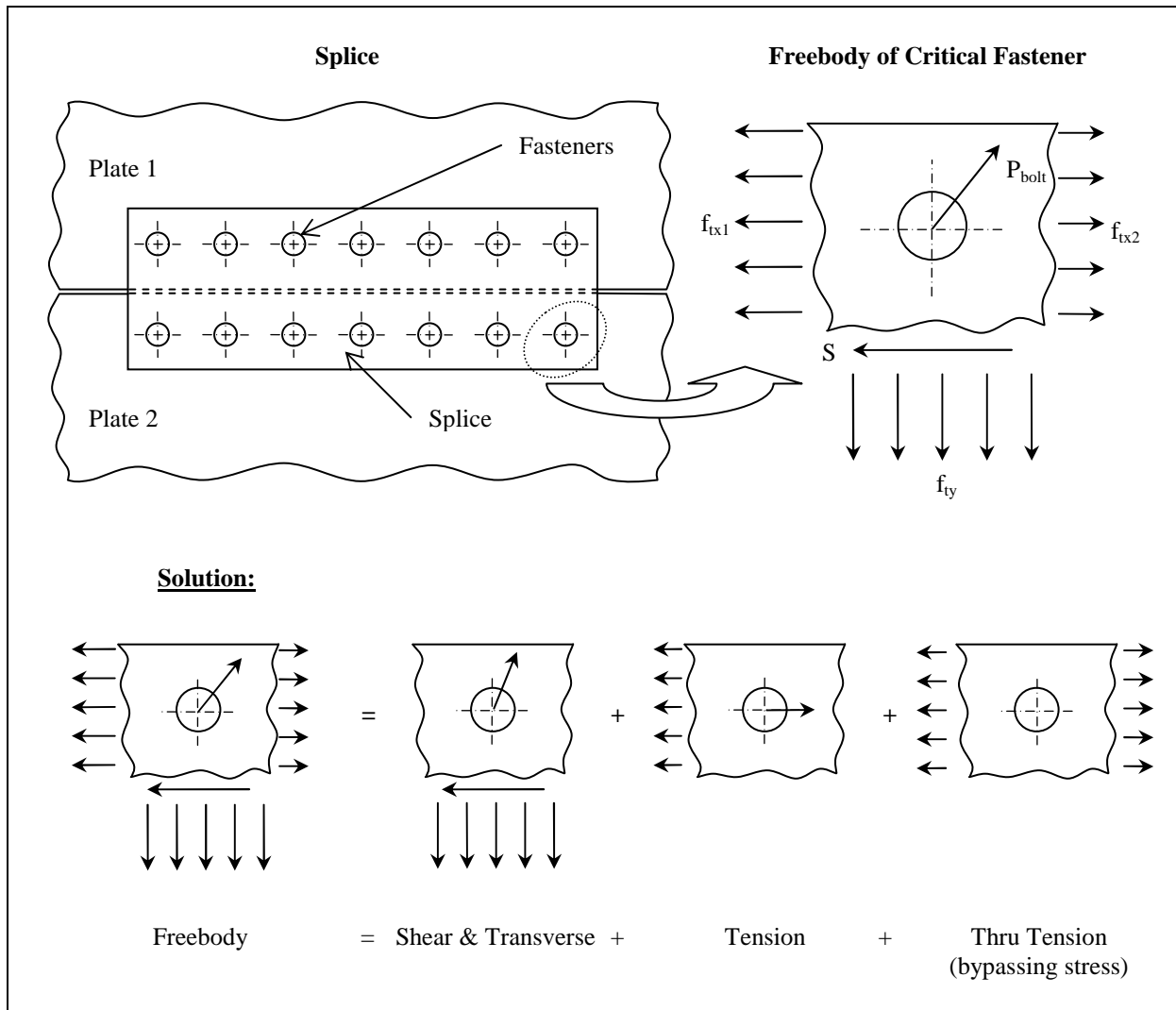


Figure 1: Breakdown of complex stress field in several standard loading cases

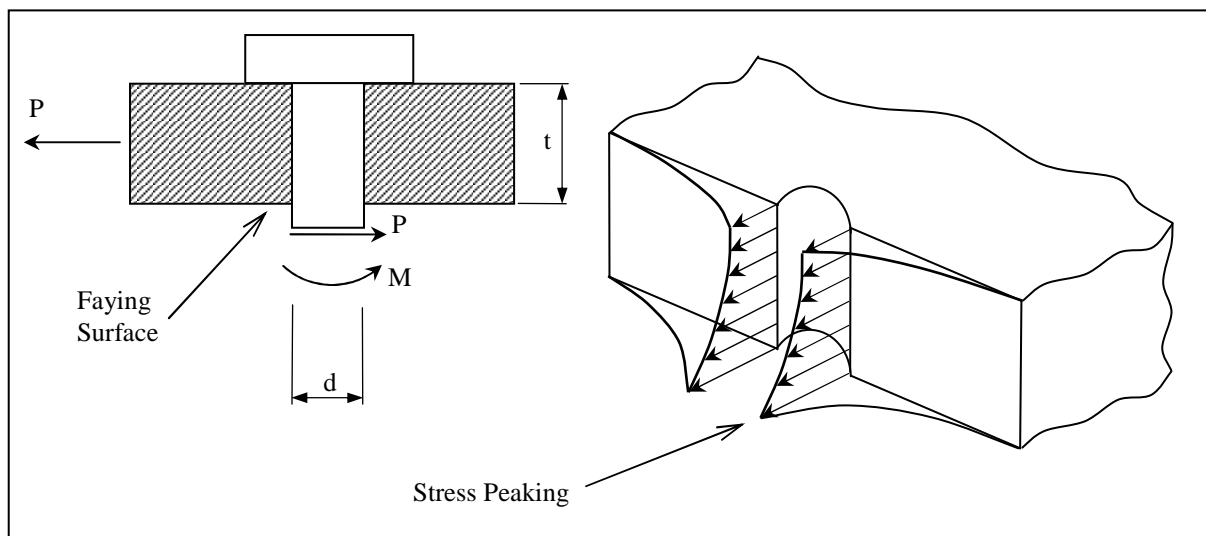


Figure 2: Stress peaking at the faying surface due to pin bending

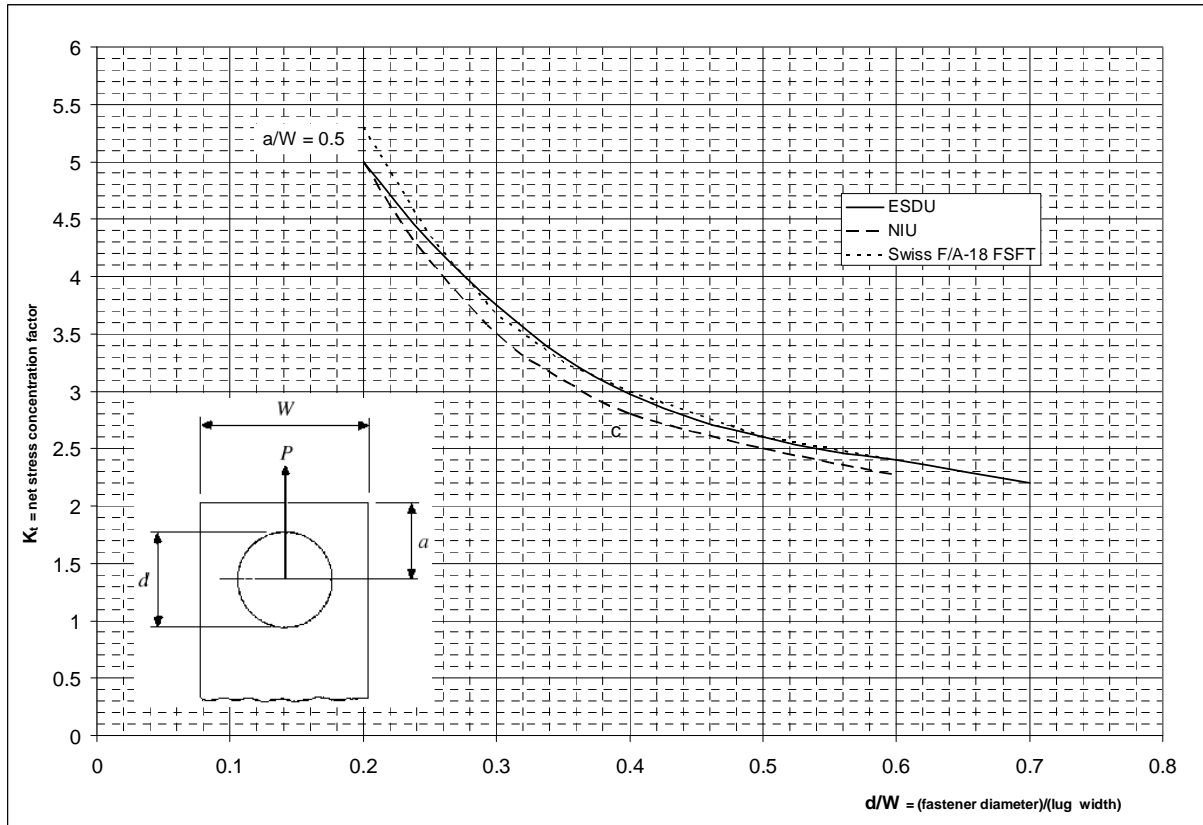


Figure 3: Net stress concentration factor in square-ended lugs, comparison between Ref. [1], [2] and [3]

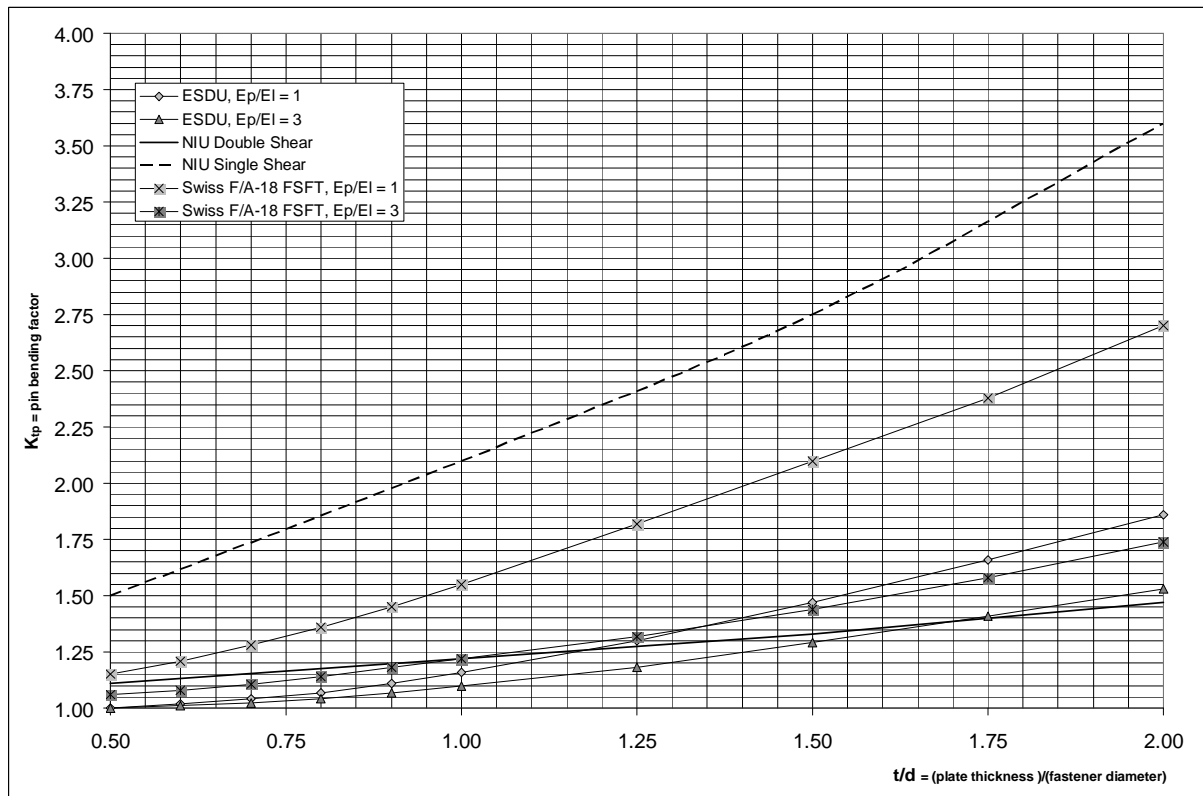
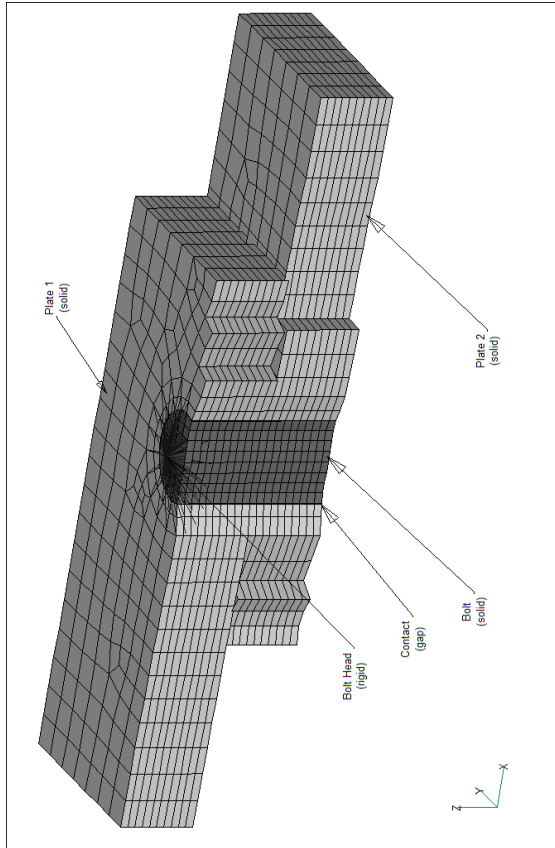
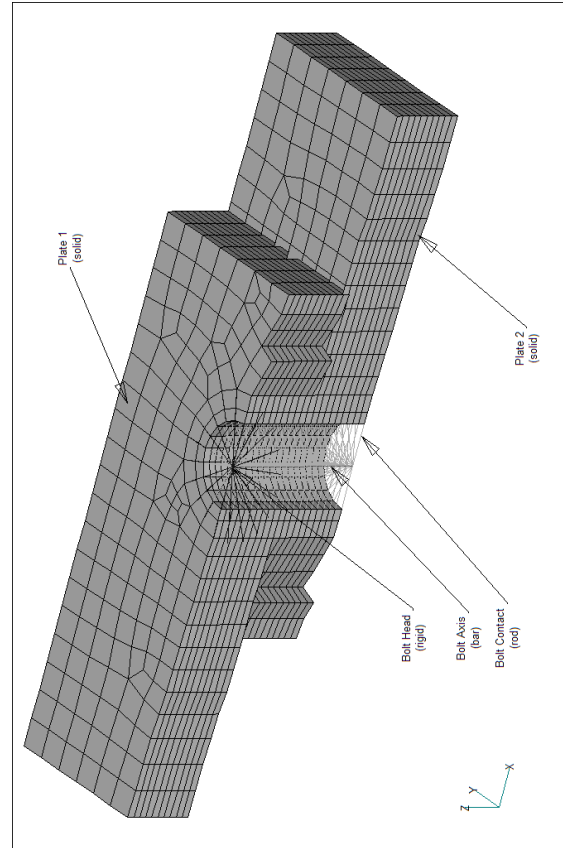


Figure 4: Pin bending factor, comparison between Ref. [1], [2] and [3]



**Figure 5:** FE Method 1 Typical Mesh



**Figure 6:** FE Method 2 Typical Mesh

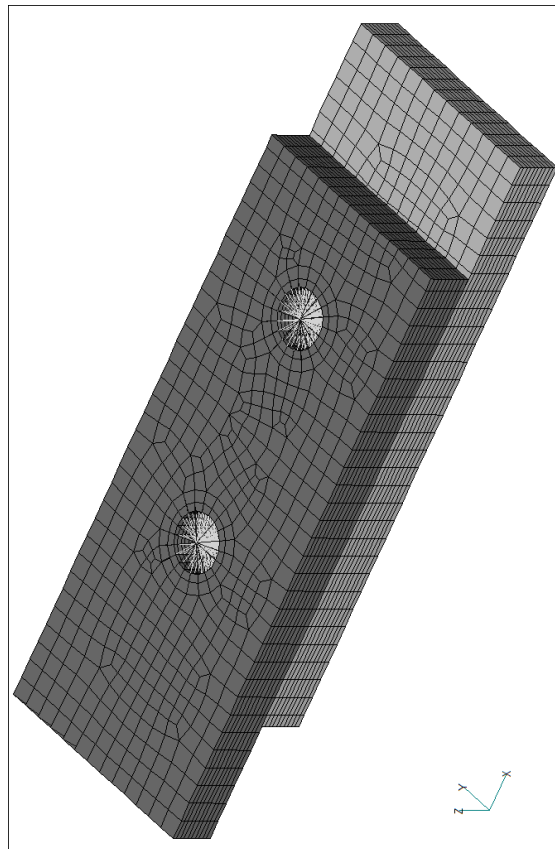


**Figure 7:** Single Lap Joint Typical Mesh

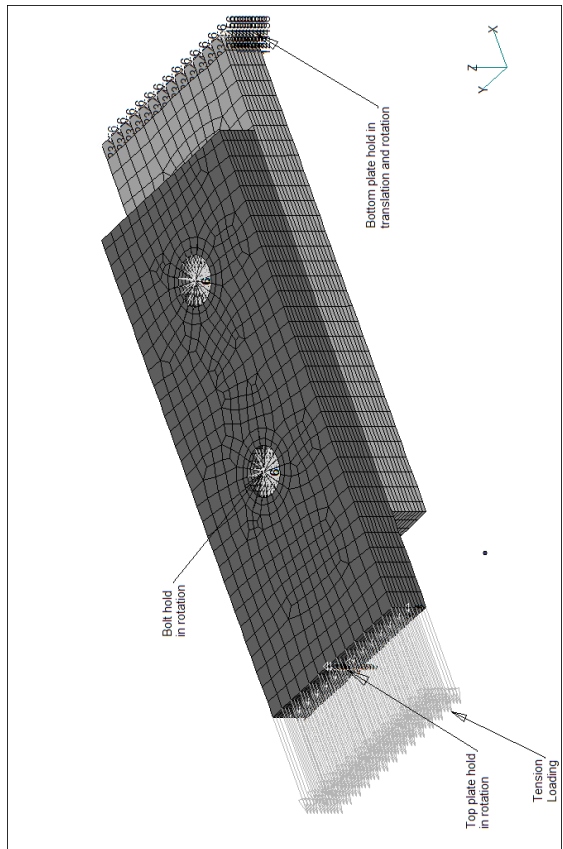


**Figure 8:** Single Lap Joint Boundary Conditions

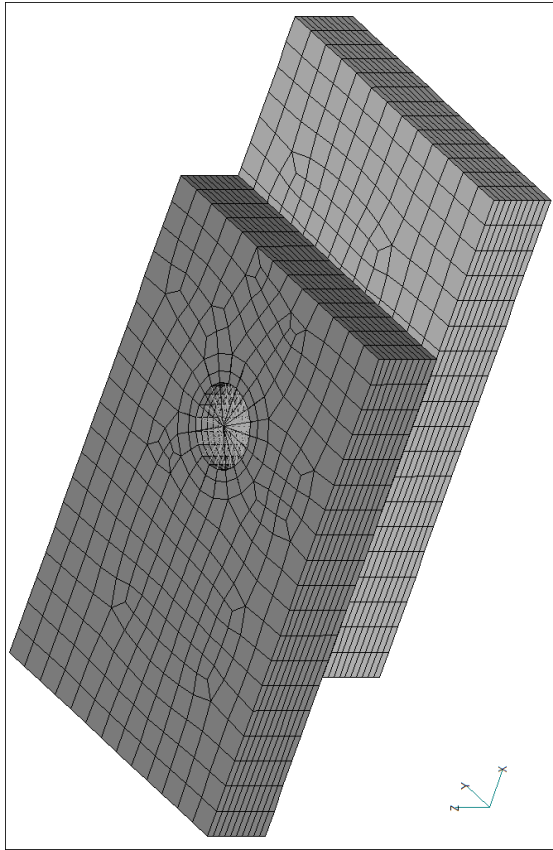


Figure 9: Double Lap Joint Typical Mesh

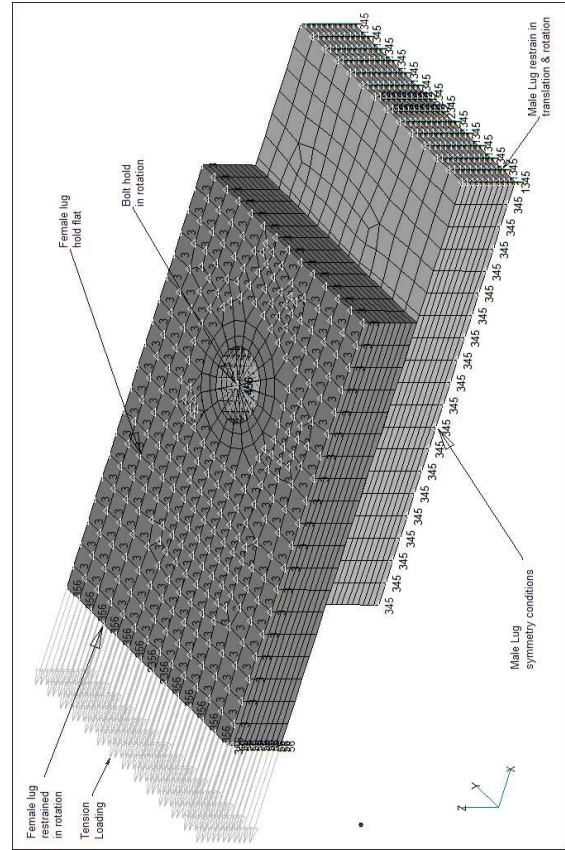


Figure 10: Double Lap Joint Boundary Conditions

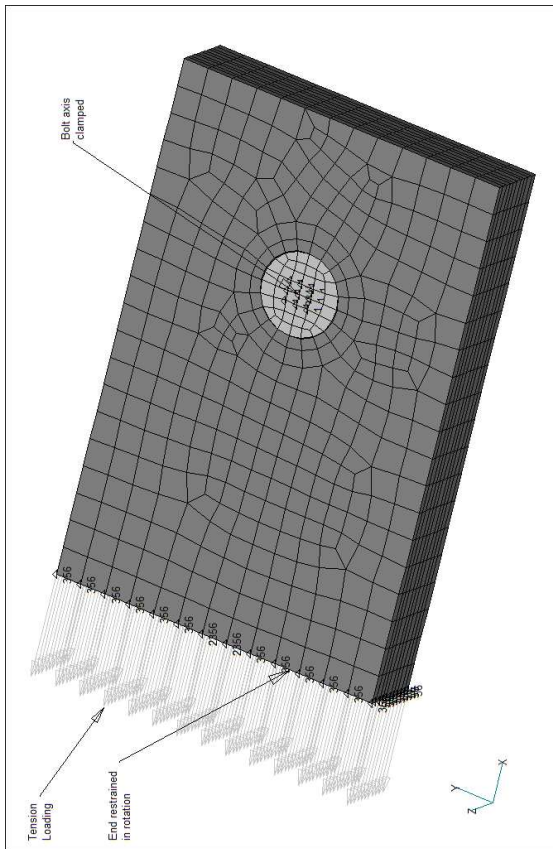


Figure 11: Square-ended Lug Mesh FE Method 1

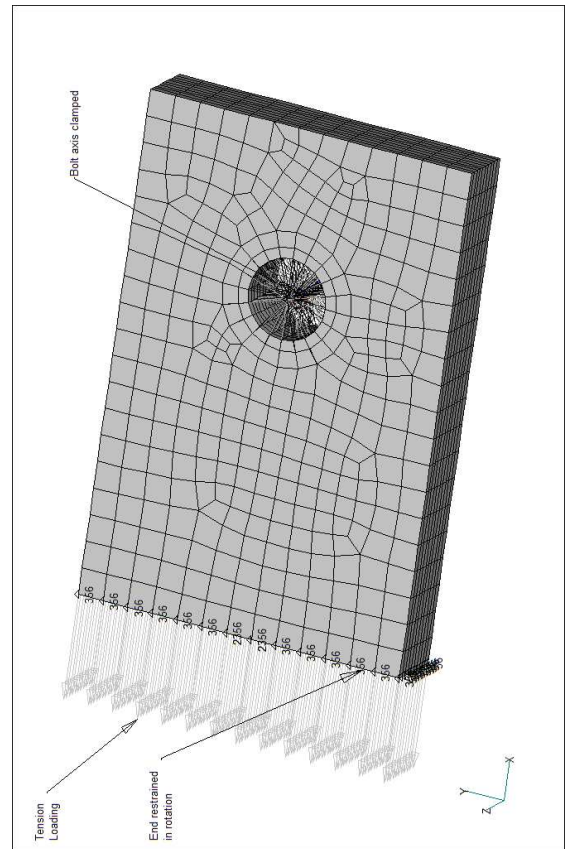


Figure 12: Square-ended Lug Mesh FE Method 2

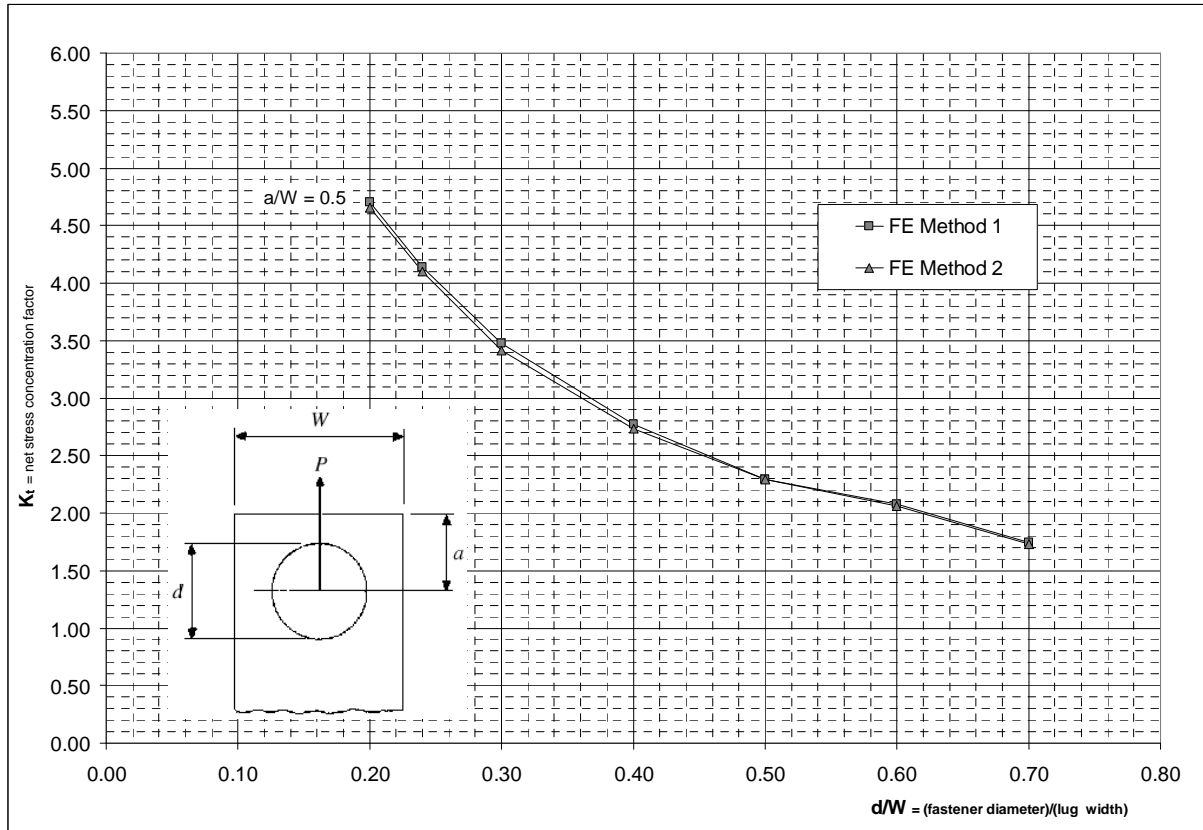


Figure 13: Net stress concentration factor in square-ended lugs, comparison between FE Methods

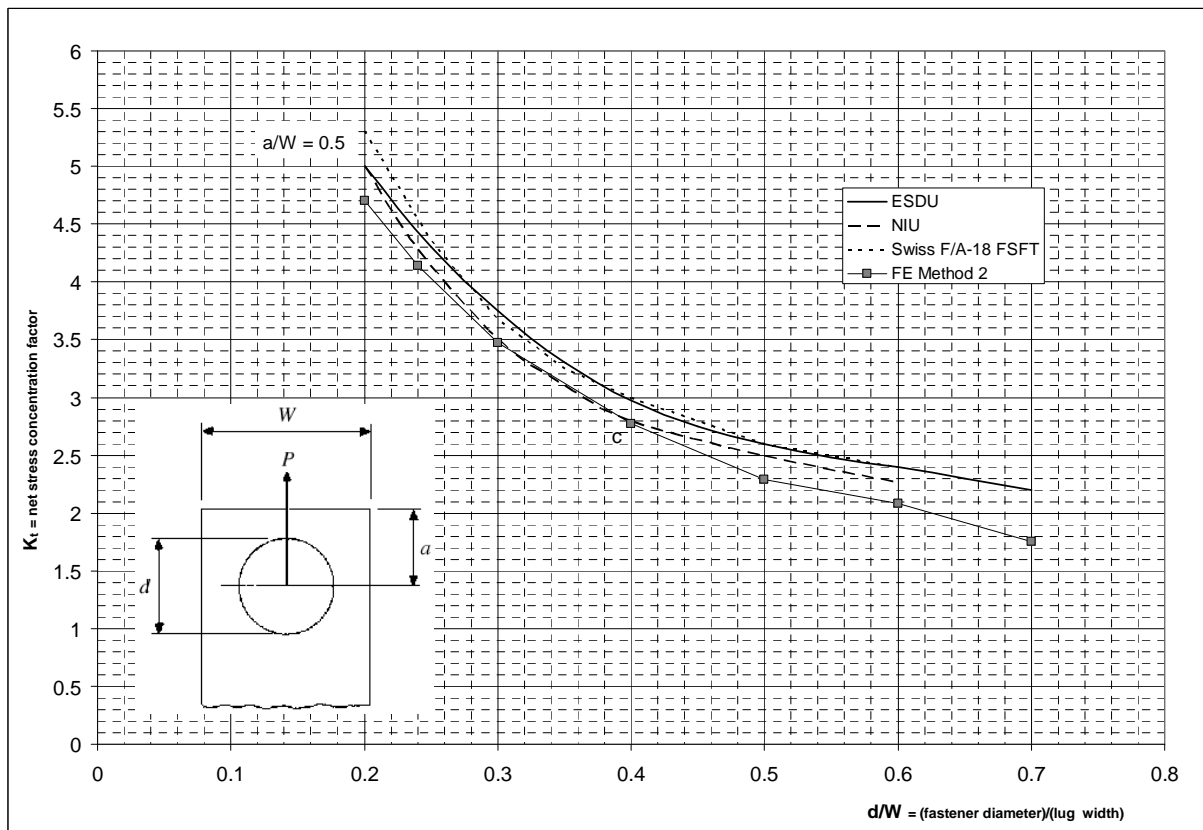


Figure 14: Net stress concentration factor in square-ended lugs, comparison between Ref. [1], [2] [3] and FE Method 2

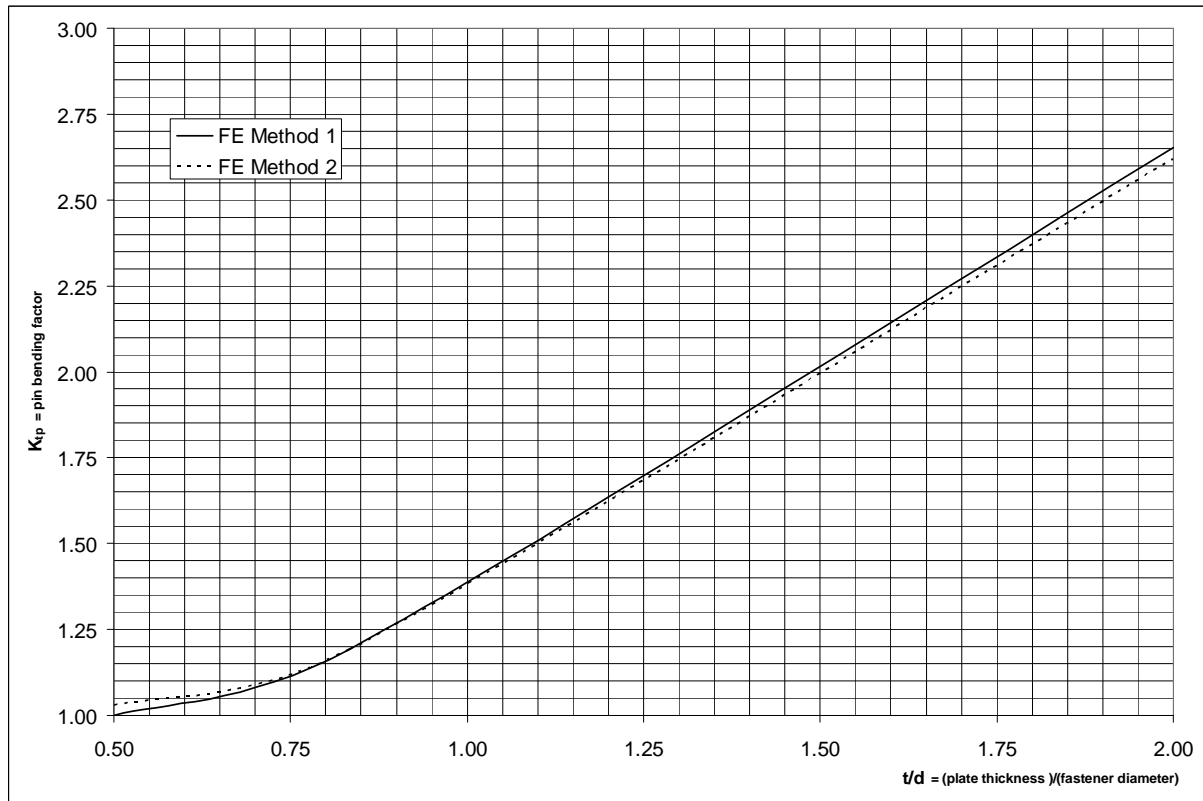


Figure 15: Pin bending factor, comparison between FE Method 1 and FE Method 2

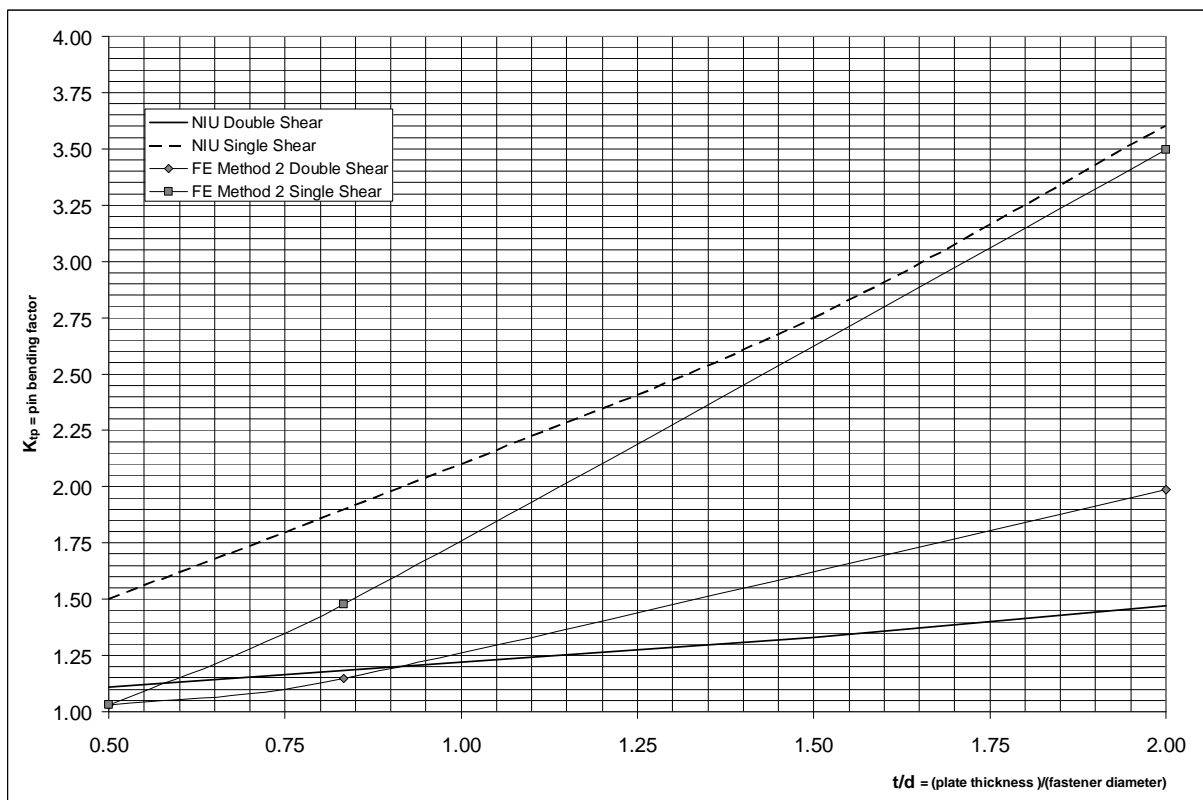


Figure 16: Pin bending factor, comparison between Ref. [2] and FE Method 2

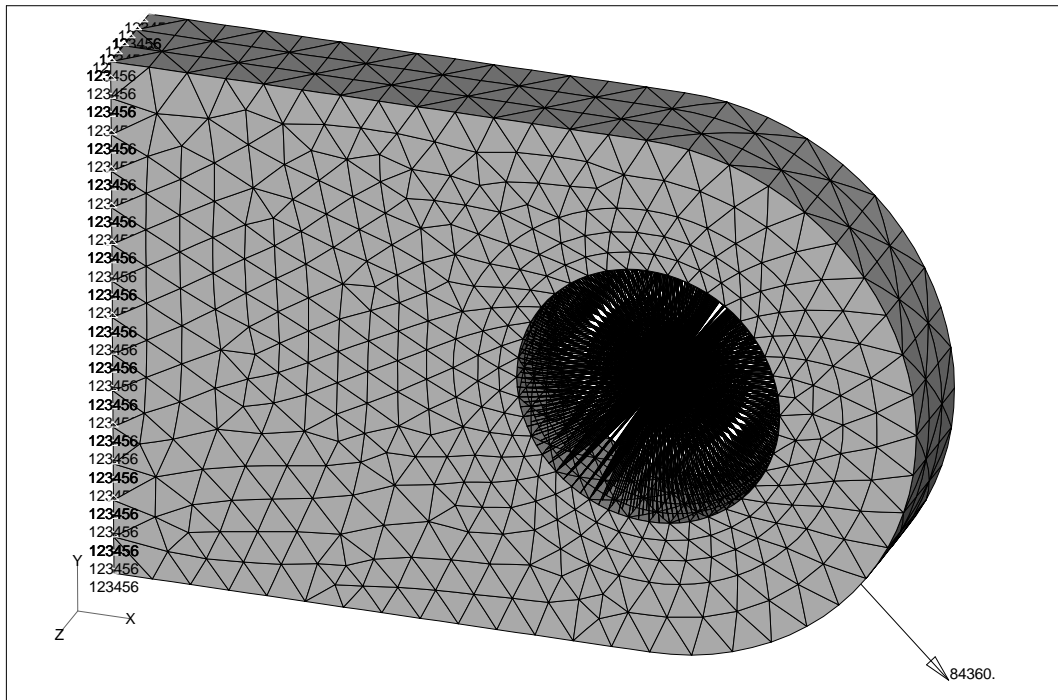


Figure 17: Round-ended Lug Mesh for Load Angle Effect Study

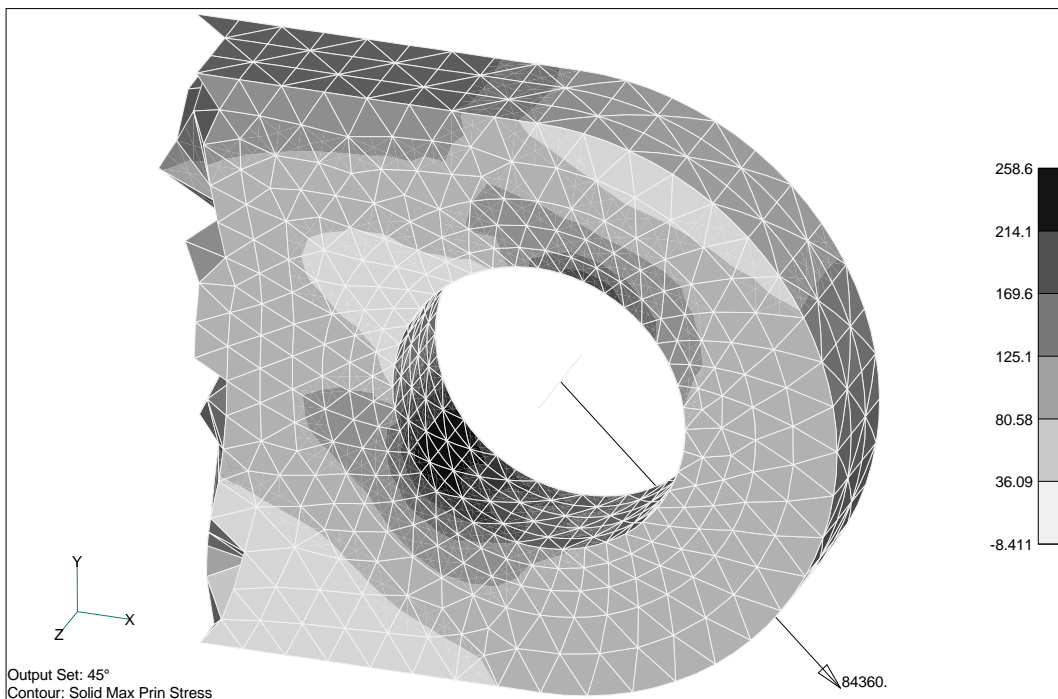


Figure 18: Round-ended Lug Stress Distribution, Load Angle = 45°

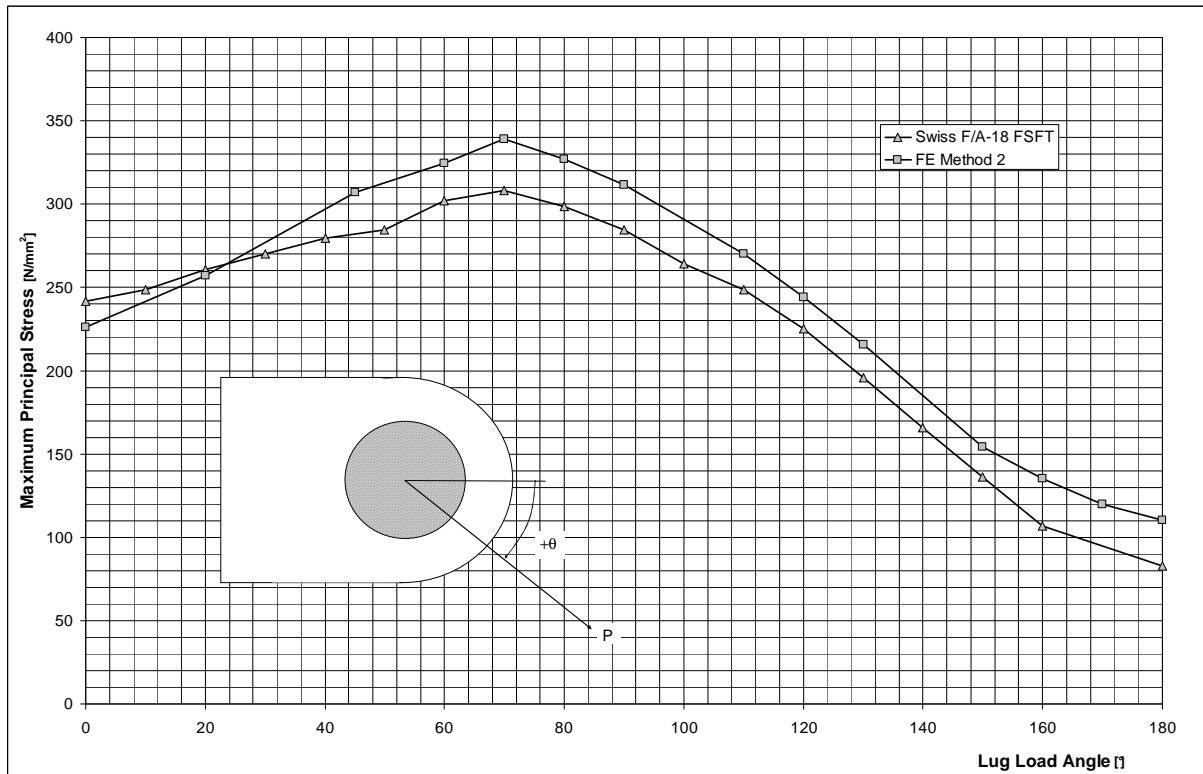


Figure 19: Loading angle influence, comparison between Ref. [3] and FE Method 2

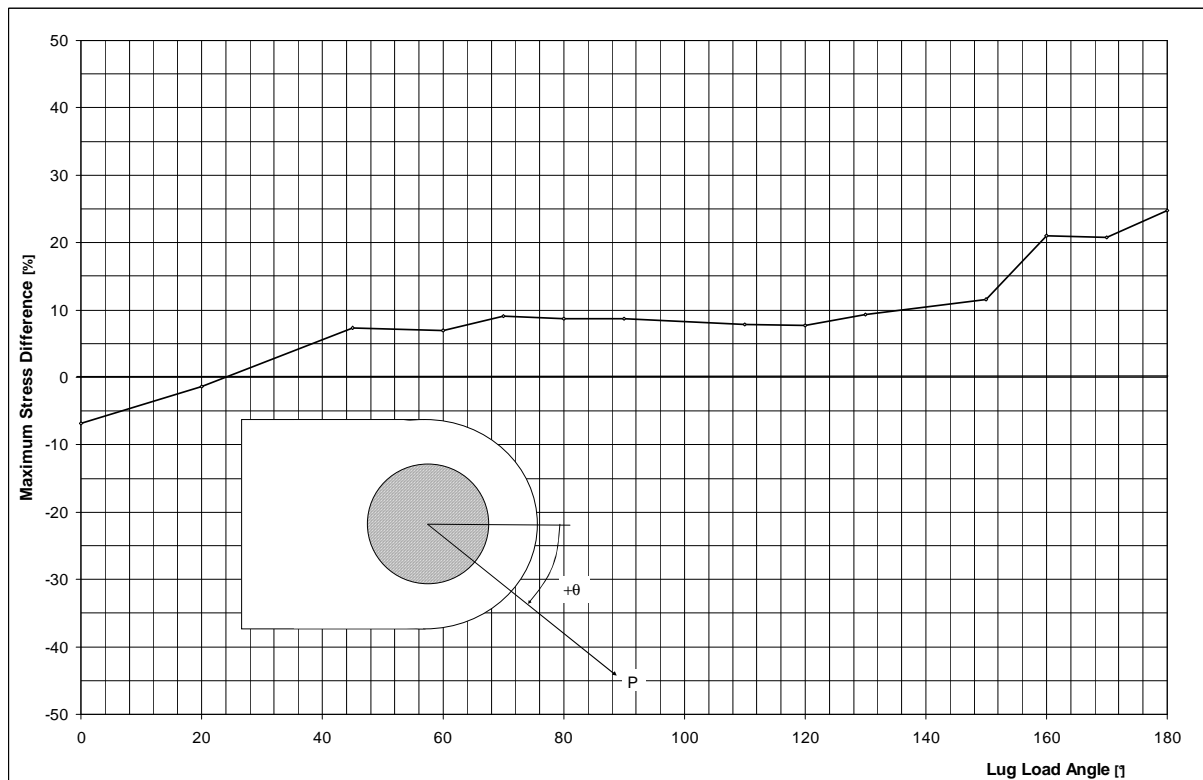


Figure 20: Loading angle influence, difference in percentage between Ref. [3] and FE Method 2

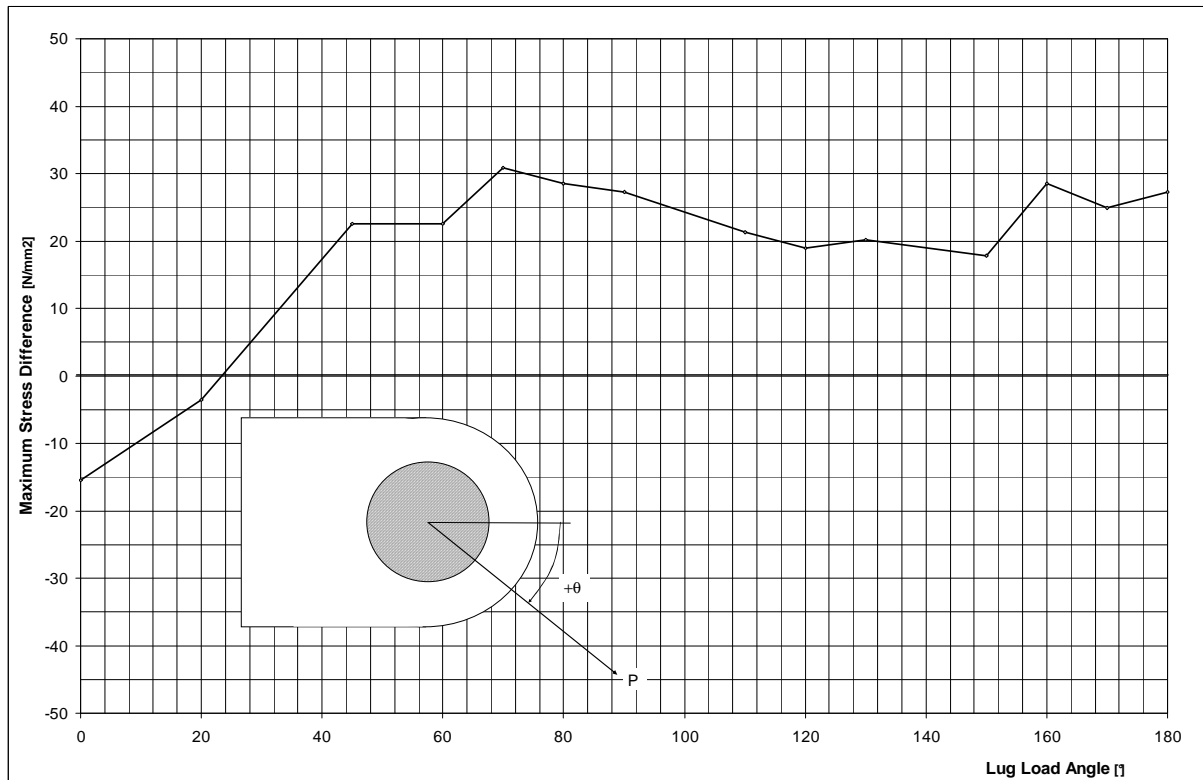


Figure 21: Loading angle influence, difference between Ref. [3] and FE Method 2

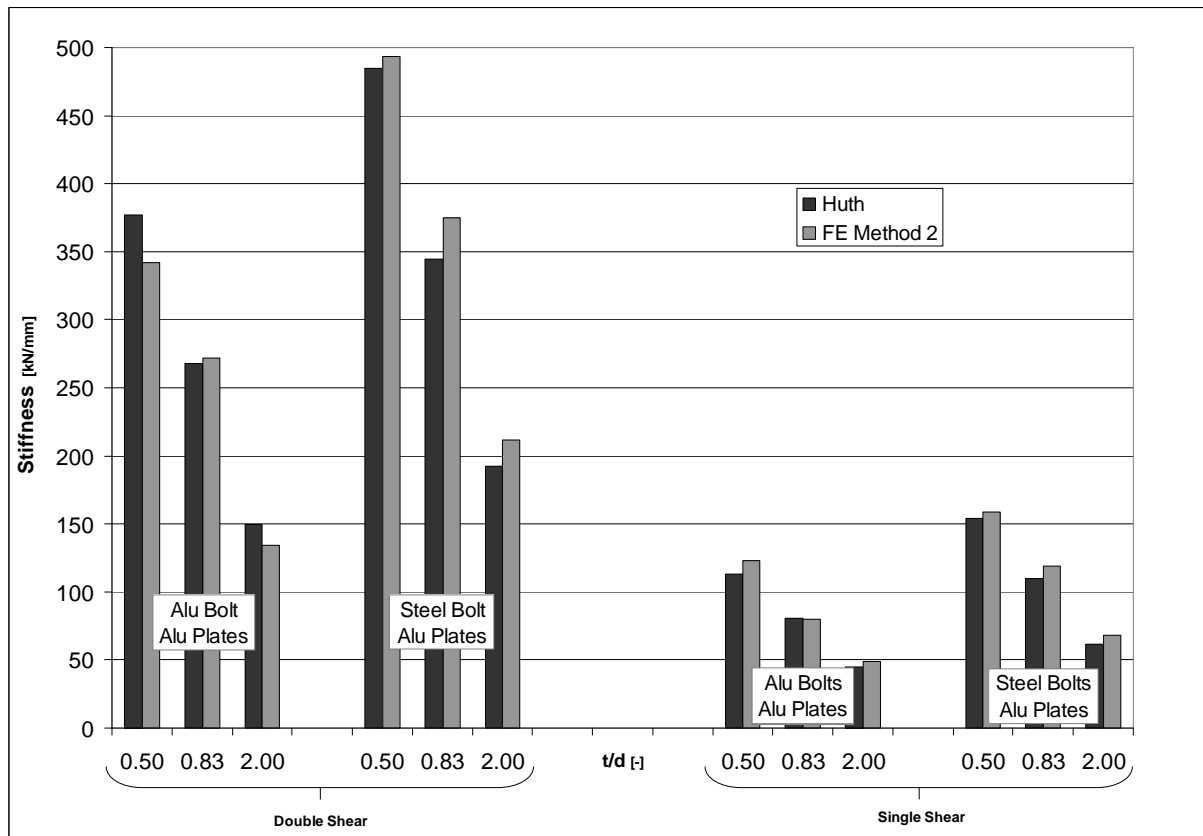


Figure 22: Connection stiffness, difference between Ref. [4] and FE Method 2

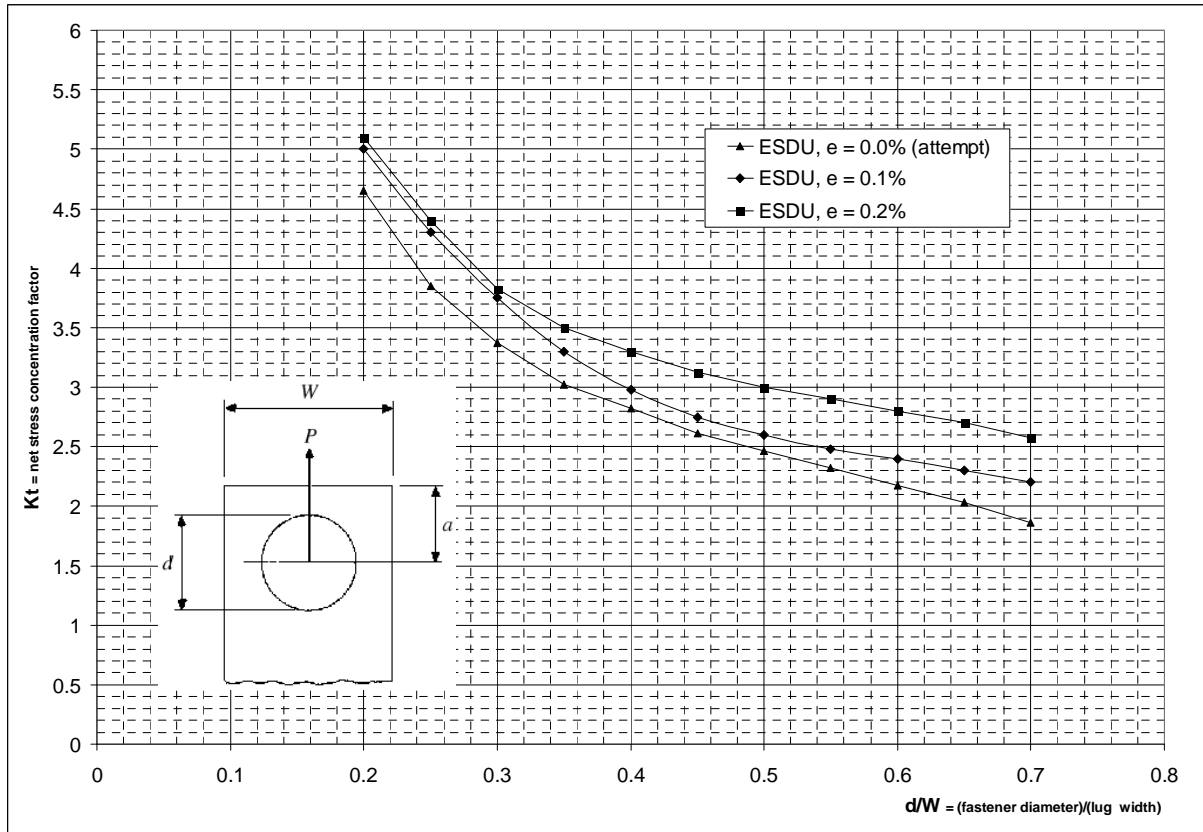


Figure 23: Impact of Clearance on the Net Stress Concentration Factor, Ref [1]

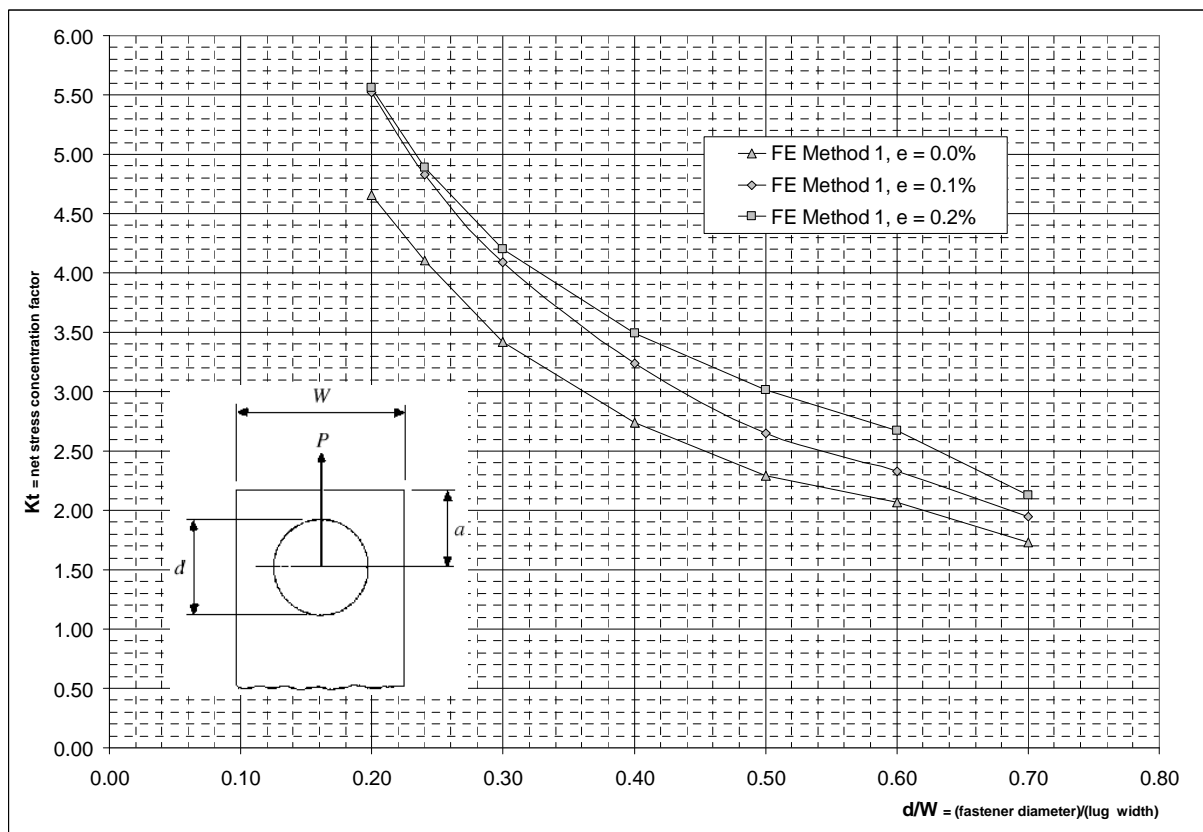


Figure 24: Impact of Clearance on the Net Stress Concentration Factor, FE Method 1

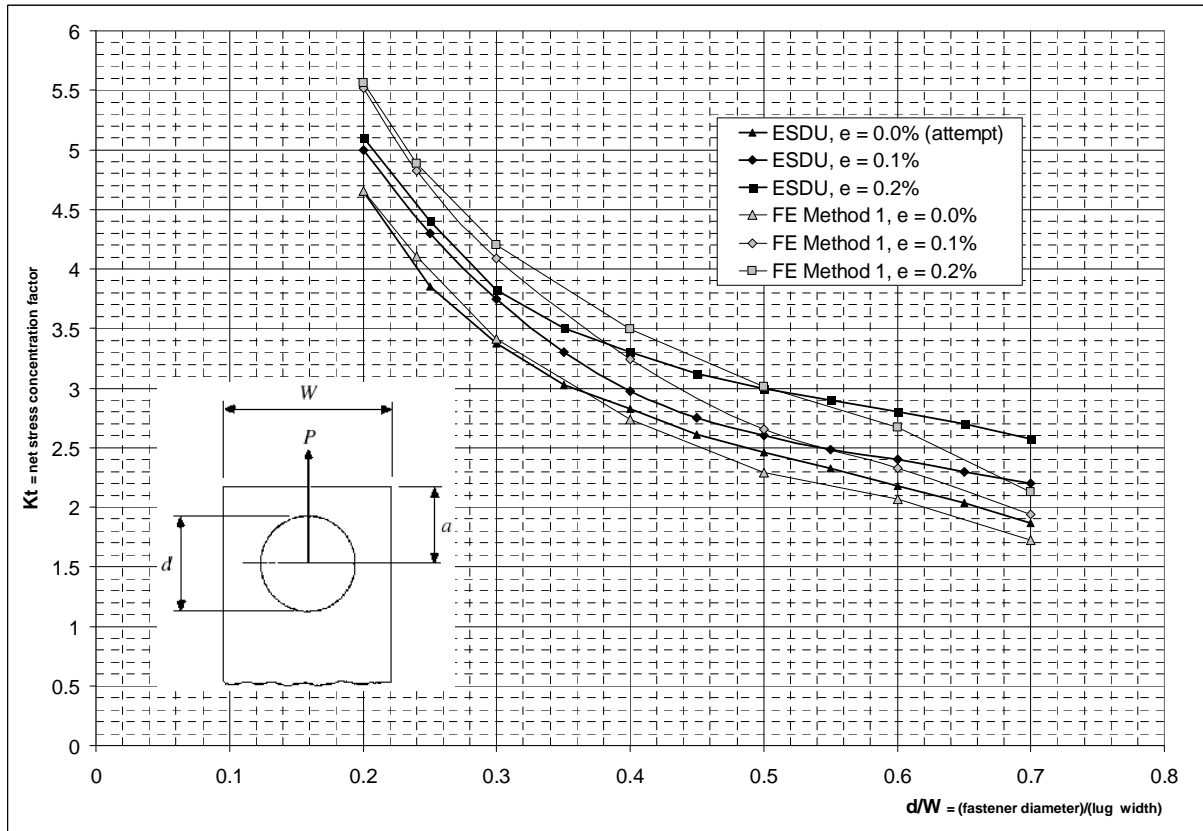


Figure 25: Impact of Clearance on the Net Stress Concentration Factor, Ref. [1] & FE Method 1

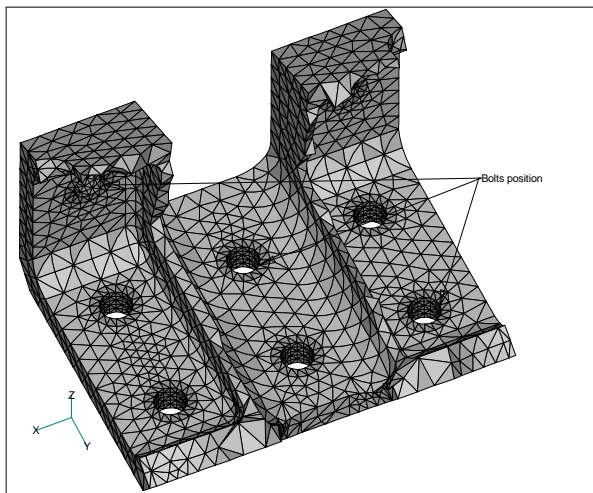


Figure 26: Typical TET10 mesh at Bolted Connection (3D Configuration)

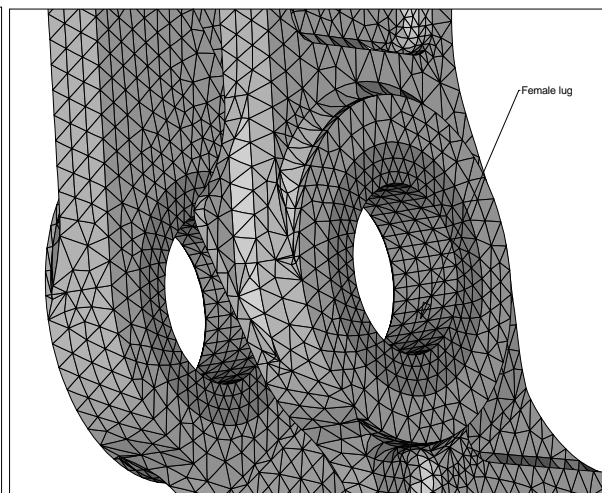


Figure 27: Typical TET10 mesh of Female Lug